FROM THE MOON TO THE EARTH WITHOUT JULES VERNE – LUNAR METEORITES AND LUNAR DUST DELIVERY. N. Artemieva[1,2], [1]Planetary Sciene Institute, artemeva@psi.edu, [2]Institute for Dynamics of Geopsheres, Russia.

Introduction: The list of lunar meteorites [1] consists of 95 names (taking into account obvious pairs) with the total mass of ~75 kg, which is approximately five times smaller than the total mass of lunar samples delivered by the *Apollo* and *Luna* missions. In contrast to "technical samples" lunar meteorites represent a random set of lunar material, including that from the far side of the Moon. Taking into account the diversity of the available lunar meteorites probably associated with various impact events [2], the short time of their transportation to Earth [3, 4], and the distribution of the crater size and age over the Moon [5], we can conclude that most of the lunar meteorites were ejected from the Moon during small impact events associated with the formation of craters of ~1 km in size [6] or even smaller [7]. This means that the corresponding projectile diameter was < 10–30 m, i.e., comparable with the lunar regolith thickness [8]. Indeed, most lunar meteorites are samples of the lunar regolith buried at the depth of 1-4 m on the Moon (2π component in CRE). However, escaping ejecta from the largest and youngest lunar craters (e.g., the 83-km Tycho crater or the 20-km Giordano Bruno crater) could represent much deeper layers and could cover the Earth with a layer of lunar rocks [9]. Such thick deposits may be found in the stratigraphic layers of a corresponding age [10] or should be presented in the lunar meteorite collections [11].

Other possible (but not as obvious as meteorites) samples of lunar material could be ^{3}He-rich dust particles in marine sedimentary rocks [12,13]. In order to transport ^{3}He from the Moon to Earth, it is necessary, first, to eject dust from the Moon at minimum compression (about 60% of the isotope is preserved in particles if they are compressed to less than 20 GPa, and the isotope is completely safe if the compression is below 10 GPa [14]); second, to not heat the dust during its deceleration in the Earth's atmosphere (the maximum temperature should be below 600°C [12]).

The spallation theory [14] and numerical simulations [6, 15-16] allowed to explain the formation of solid high-velocity ejecta and to reconcile the results of numerical models with observations. However, relative deficiency of lunar meteorites compared with the Martian ones has not been explained yet. The main goal of this study is to re-evaluate the amount of escape ejecta from the Moon taking into account the highly porous upper regolith layer. The porosity may be relevant in two ways. First, the impact pressure required to melt porous materials, is much lower than 50 -60 GPa [17]. Second, the spall effect is noticeably weaker in porous media [15, 18]. Another goal is to evaluate the total mass and ^{3}He losses in the terrestrial atmosphere during the entry process. Mass losses may be as high as 90% in typical meteorites [19].

Numerical model and initial conditions: High-velocity impacts on the Moon are modeled using the 3D hydrocode SOVA [20] complemented by the ANEOS equation of state for geological materials [21]. The lunar regolith porosity is described in the frame of ε-alpha model [22].Tracer particles are used to find the maximum shock compression and the initial depth of solid ejecta escaping the Moon (SEEM). Entry of SEEM into the atmosphere is described within the point mass approximation [23] for bodies larger than 1 cm or as a free molecular flow for smaller bodies [24].

Typical impact parameters (dunitic composition, 18 km/s at 45° to horizon) are used for projectiles with diameters from 1 to 500 m. The target consists of lunar soil with density ρ increasing with depth *Z* (in cm) according to the equation $\rho=\rho_0+0.121 ln\ (Z+1)$ with $\rho_0=1.38$ g/cm^3 [25]. Entry velocities in the atmosphere vary from 11.5 km/s to 18 km/s, particle sizes – from 1 μm to 50 cm.

Departure from the Moon: Presence of a porous regolith layer decreases the total mass of SEEM – from 1 projectile mass after an impact into consolidated non-porous target to 0.06*M* after an impact into a pure regolith layer with a constant density of 1.6 g/cm^3. This dramatic, almost twentyfold, decrease is mainly related to substantial decrease in the value of shock pressure causing rock melting– from 60 GPa in solid rocks to 15 GPa in 40% porous regolith. As a result, in nonporous rocks 55% of all escape ejecta are solid, while in porous rocks this parameter is below 10%. The modeled dependence of SEEM on the projectile mass for the realistic density profile is summarized in the Table:

D_{pr}, m	M_{SEEM}/M_{pr}	Depth/D
small	0.06	0.11
50	0.35	0.15
100	0.38	0.16
500	0.68	0.20
>500	1.02	0.23

The excavation depth of SEEM does not exceed 10-20% of the projectile diameter (see Fig. 2), i.e., is substantially smaller than the total excavation depth (1/10 of crater diameter) as it was assumed in [7]. For

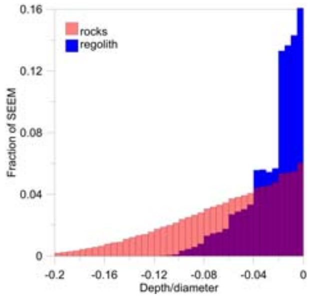

example, a 10-m projectile excavates SEEM from the depth of ~1-2 m, but makes a ~1-km-diameter crater with the total excavation depth of about 80 m.

Fig. 1 (left). Distribution of SEEM over depth.

Fig. 2 (right). View from the sky to the impact site of a 50-m-diameter projectile. The impact is at the point (0, 0) - outside the frame. The upper plate shows ejection velocities, the bottom plate – the values of maximum shock compression. Relatively low spatial resolution (25 cells per radius) does not allow to resolve SEEM with low (<15 GPa) shock compression and, hence, enriched in ^{3}He.

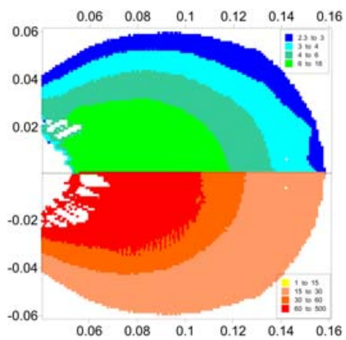

As a rule, regolithic SEEM have lower velocities than SEEM from consolidated rocks: 78% and 40%, respectively, have velocities below 2.8 km/s and remain in the Earth's gravitational field.

The amount of ejecta enriched in ^{3}He nearly coincides with the total amount of SEEM for small, <10 m in diameter projectiles, and is proportional to the projectile volume. For larger projectiles this volume increases as squared projectile diameter as only the upper few meters of the Moon are enriched in ^{3}He.

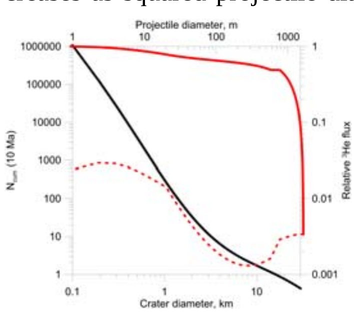

Fig. 3. 10 Myr time interval: cumulative distributions of lunar craters (black line, left axis) and escaping ^{3}He (red line, right axis).

Arrival to the Earth: Large (>1 cm) particles lose 20 – 50% (entry velocities 11.4 – 18 km/s) of their initial mass due to ablation, but remain cold inside. Smaller particles (<1 mm) are isothermal and are heated to 1700, 980, and 500 K. (diameters 100, 10, and 1 μm, respectively – see Fig. 4). As 10% of lunar soil particles are smaller than 10 μm (they are also the richest in ^{3}He), these particles can deliver ^{3}He to the Earth without substantial loss.

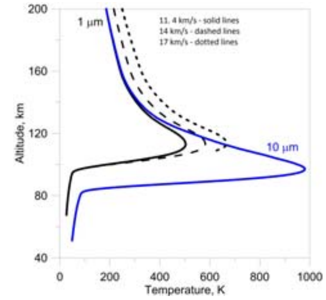

Fig. 4. Temperature of 1 and 10 μm particles as a function of altitude for various entry velocities (11.4 – 17 km/s). Only variants with T_{max} < 1000 K) are shown.

Discussion: *NWA5000.* Projectiles smaller than 10-20 m in diameter are able to propel exclusively the regolith (i.e., dust with random and unknown inclusions of consolidated breccia or rocks) into space. It means that the contribution of these small cratering events to the flux of lunar meteorites is sporadic. Larger impact events are statistically unlikely within a short (< 10 kyr) time frame [5]. Thus, the biggest (11.5 kg) and the youngest (<10 kyr) lunar meteorite, NWA5000 (feldsparic breccia) is a real miracle.

^{3}He in stratigraphic layers. Although small impacts are the most efficient source of ^{3}He on a long time interval (Fig. 3), any large impact on the Moon creates a strong peak in sedimentary records within a short time interval (~a few thousand years).

References: [1] http://meteorites.wustl.edu/lunar/moon_meteorites.htm. [2] Korotev R.L. (2005) *Chem. Erde*, *65*, 297–346. [3] Serefiddin F. et al. (2011) LPS-42, Abstract # 1392. [4] Gladman B.J. (1995) *Icarus*, *118*, 302–321. [5] Neukum G. et al. (2001). *Space Sci. Rev.*, *96*, 55–86. [6] Artemieva N. and Ivanov B. (2004) *Icarus*, *171*, 84–101. [7] Basilevsky A. et al. (2010) *Planet. Space Sci.*, *58*, 1900-1905 [8] Oberbeck V.R. (1973) *Icarus*, *19*, 87–107. [9] Artemieva N. (2013) *LPS-44*, Abstract #1413. [10] Schmitz B. et al. (2001) *Earth Planet. Sci. Lett.*, *194*, 1–15. [11] Fritz J. (2012). *Icarus*, *221*, 1183-1186. [12] Farley K.A. (1997) et al. *Geochim. Cosmochim. Acta*, *61*, 2309–2316. [13] Fritz J. (2007) *Icarus*, *189*, 91–594. [14] Schwenzer S. P. et al. (2008) *M&PS*, *43*, 1841-1859. [14] Melosh H.J. (1984) *Icarus*, *59*, 234-260. [15] Head et al. (2002) *Science*, 298, 1752–1756. [16] Artemieva N. and Shuvalov V. (2008) *Solar System Res.*, *42*, 329–334. [17] Wünnemann K. et al. (2008) *E&PSL*, *269*, 530-539. [18] Collins G., and Wünnemann K. (2007) *Bridging the Gap II*, 35-36. [19] Ceplecha R. and ReVeller D.O. (2005) *M&PS*, *40*, 35–54. [20] Shuvalov V. (1999) *Shock waves 9*, 381-390. [21] Melosh H.J. (2007) *M&PS*, *42*, 2079-2098. [22] Wünnemann K. et al. (2006) *Icarus*, *180*, 514-527. [23] Artemieva N. and Shuvalov V. (2001). *JGR*,*106*, 3297-3310. [24] Love S.G. and Brownlee D.G. (1993) *Icarus*, *9* 26-43. [25] Lindsey J. (1976) *Lunar stratigraphy and sedimentology*, 311 p.